

Do We Really Need a Learnable Classifier at the End of Deep Neural Network?

Yibo Yang¹, Liang Xie², Shixiang Chen¹, Xiangtai Li³, Zhouchen Lin³, Dacheng Tao¹

¹JD Explore Academy, Beijing, China

²State Key Lab of CAD&CG, Zhejiang University, Hangzhou, China

³Key Laboratory of Machine Perception (MOE), School of AI, Peking University, Beijing, China

March 18, 2022

Abstract

Modern deep neural networks for classification usually jointly learn a backbone for representation and a linear classifier to output the logit of each class. A recent study has shown a phenomenon called *neural collapse* that the within-class means of features and the classifier vectors converge to the vertices of a simplex equiangular tight frame (ETF) at the terminal phase of training on a balanced dataset. Since the ETF geometric structure maximally separates the pair-wise angles of all classes in the classifier, it is natural to raise the question, *why do we spend an effort to learn a classifier when we know its optimal geometric structure?* In this paper, we study the potential of learning a neural network for classification with the classifier randomly initialized as an ETF and fixed during training. Our analytical work based on the layer-peeled model indicates that the feature learning with a fixed ETF classifier naturally leads to the neural collapse state even when the dataset is imbalanced among classes. We further show that in this case the cross entropy (CE) loss is not necessary and can be replaced by a simple squared loss that shares the same global optimality but enjoys a more accurate gradient and better convergence property. Our experimental results show that our method is able to achieve similar performances on image classification for balanced datasets, and bring significant improvements in the long-tailed and fine-grained classification tasks.

1 Introduction

Modern deep neural networks for classification are composed of a backbone network to extract features, and a linear classifier in the last layer to predict the logit of each class. Although the backbone network architecture has not been interpretable enough with respect to performance, generalization, and robustness, its aim for classification is rather clear, which is to produce features that are as linearly separable as possible, so the last-layer linear classifier could separate features and make predictions. For decades, as widely adopted in nearly all deep learning fields, the linear classifier has been learnable jointly with the backbone network using the cross entropy (CE) loss function for classification problems [1, 2, 3].

A recent study reveals a very symmetric phenomenon, named neural collapse, that the last-layer features of the same class will collapse to their within-class mean, and the within-class means of all classes and their corresponding classifier vectors will converge to the vertices of a simplex equiangular tight frame (ETF) with self-duality at the terminal phase of training on a balanced dataset [4]. A simplex ETF describes a geometric structure that maximally separates the pair-wise angles of

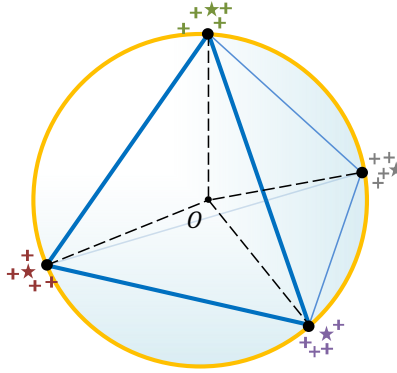


Figure 1: An illustration of a simplex equiangular tight frame when $d = 3$ and $K = 4$. The black spheres are the vertices of the ETF. The “+” and asterisks signs in different colors refer to features and classifier vectors of different classes, respectively. Neural collapse depicts the phenomenon that the last-layer feature means and the corresponding classifier vectors converge to the same ETF.

K vectors in \mathbb{R}^d , $d \geq K - 1$, and all vectors have equal ℓ_2 norms. As shown in Figure 1, when $d = K - 1$, the ETF reduces to a regular simplex. Following studies focus on unveiling the physics of such a phenomenon. Some studies propose to analyze a surrogate model, named layer-peeled model (LPM) [5] or unconstrained feature model [6], by peeling off the topmost layer, so the features are independent variables to optimize [7]. Although this toy model is impracticable for application, it inherits the nature of feature and classifier learning in real deep networks. It has been shown that the optimality for LPM under the CE loss leads to the neural collapse solution with feature norm constraints [8, 5, 7, 9], regularization [10], or even no explicit constraint [11]. Other studies turn to analyze the unconstrained LPM under the mean squared error (MSE) loss and also derive the neural collapse solution [6, 12, 13, 14].

Albeit neural collapse is an observed empirical result and has not been entirely understood from a theoretical point, it is intuitive and sensible. Features collapsing to their means minimize the within-class variability, while the ETF geometric structure maximizes the between-class variability, so the Fisher discriminant ratio [15, 16] is maximized, which corresponds to an optimal linearly separable state for classification. Several works have shown that neural networks progressively increase the linear separability during training [17, 18, 19]. Therefore, a classifier that satisfies the ETF structure should be a “correct” answer for network training. However, as pointed out by [5], in the training of an imbalanced dataset, the classifier vectors of the minority classes will merge, termed as *minority collapse*, which breaks up the ETF structure and deteriorates the performance on test data. So a learnable classifier does not always lead to neural collapse and may increase the coupled optimization difficulty. With the spirit of *Occam’s Razor* [20], we raise and study the question: *do we really need to learn a linear classifier at the end of deep neural network for classification?*

Since a backbone network is usually over-parameterized and can produce a feature align with any direction, what matters for classification should be the feature-classifier geometric structure, instead of their specific directions. In this paper, we propose to initialize the classifier using a randomly generated ETF and fix it during training, *i.e.*, only the backbone network is learnable. It turns out that this practice makes the LPM more mathematically tractable as a convex problem. Our analytical work indicates that even in the training of an imbalanced dataset, the features will converge to the vertices of the same ETF as the fixed classifier, so neural collapse emerges inherently regardless of class balance.

We further rethink the cross entropy loss function. We point out the reason for minority collapse from the perspective of imbalanced gradients with respect to a learnable classifier. As a comparison, our fixed ETF classifier does not suffer from this dilemma. We also show that the gradients with

respect to the last-layer feature are composed of a “pull” term that pulls the feature into the direction align with its corresponding classifier vector, and a “push” term that pushes it away from the other classifier vectors. It is the pull-push mechanism in the CE loss that makes the feature and classifier of different classes separated and form into the ETF structure. However, in our case, the classifier has been fixed as a “correct” answer. As a result, the “pull” term is an accurate gradient towards the optimality, and we no longer need the “push” term that may cause inaccurate gradients. Inspired by the analyses, we further propose a simple squared loss, named dot regression (DR) loss, that shares a similar “pull” gradient as the CE loss but does not have any “push” term. It has the same global optimality as the CE loss in the LPM, but enjoys a better convergence property.

The contributions of this study can be listed as follows:

- We propose a new paradigm for deep neural network with the linear classifier randomly initialized as a simplex ETF and fixed during training. Our analytical work based on the layer-peeled model shows that this implementation is able to produce the neural collapse optimality even when the dataset is imbalanced.
- We point out that our fixed ETF classifier no longer needs the “push” gradient *w.r.t* feature that is crucial for the CE loss but may be inaccurate. We further propose a simple loss function that only has the “pull” gradient. Its better convergence property is theoretically proved.
- Experimental results show that our method is able to improve the performance of classification with imbalanced training data, *i.e.*, long-tailed classification, by a significant margin. As an extension, we show that our method also works for fine-grained classification.

2 Related Work

2.1 Neural Network for Classification

Deep neural network has been a strong tool for the classification problem [1]. A lot of architectures have been proposed for the backbone network to improve the performance [21, 2, 3, 22]. Despite the success, a theoretical foundation for neural architecture in terms of learning ability, generalization, and robustness still remains an open problem and inspires many studies from different perspectives [23, 24, 25, 26]. Compared with the complex backbone network, the linear classifier in the last layer has been rather transparent. In most cases, it is jointly optimized with the backbone network. In the long-tailed classification problem, a two-stage training method has been popular [27, 28, 29]. The first stage trains the model using instance-balanced data, while the second stage only finetunes or learns a weight scaling for the classifier using class-balanced data. Different from these studies, we study the potential of using a fixed classifier throughout the training. We also show some theoretical merits of our methods in the long-tailed classification case.

2.2 Neural Collapse

In [4], the authors reveal an empirical observation that the features will collapse to their within-class means, and the means together with the classifier vectors will converge to a simplex equiangular tight frame at the terminal phase of training on a balanced dataset. Albeit the phenomenon is intuitive, its reason has not been entirely understood, which inspires several lines of theoretical work on it. [4] proves that if features satisfy neural collapse, the optimal classifier vectors under the MSE loss will also converge to neural collapse based on the result in [30]. Some studies turn to a simplified model that only considers the last-layer features and the classifier vectors as independent variables [7, 5, 8, 10, 11, 9]. They prove that neural collapse emerges under the CE loss with proper constraint or regularization. Other studies prove that the MSE loss also leads to the neural collapse solution [6, 12, 13, 14]. [31] proposes a convex formulation for a norm-regularized ReLU network and explains

neural collapse accordingly. However, most of these results are based on the balanced training. In [10], they tried the practice of fixing the last-layer linear classifier as a simplex ETF in experiment, but did not provide any theoretical or experimental merit except for the saved computation cost. Our work differs from these studies in that we theoretically show that neural collapse can inherently happen even in the imbalanced training with a fixed ETF classifier. We also derive a new loss function specified for this practice with better convergence property than the CE loss.

3 Preliminaries

In this section, we offer a brief review of neural collapse and the analytical framework, layer-peeled model (LPM).

3.1 Neural Collapse

[4] reveals an empirical phenomenon, termed as neural collapse (NC), that the last-layer features converge to their within-class means, and the within-class means together with the classifier vectors collapse to the vertices of a simplex equiangular tight frame (ETF) at the terminal phase of training on a balanced dataset.

Definition 1 (Simplex Equiangular Tight Frame) A collection of vectors $\mathbf{m}_i \in \mathbb{R}^d$, $i = 1, 2, \dots, K$, $d \geq K - 1$, is said to be a simplex equiangular tight frame if:

$$\mathbf{M} = \sqrt{\frac{K}{K-1}} \mathbf{U} \left(\mathbf{I}_K - \frac{1}{K} \mathbf{1}_K \mathbf{1}_K^T \right), \quad (1)$$

where $\mathbf{M} = [\mathbf{m}_1, \dots, \mathbf{m}_K] \in \mathbb{R}^{d \times K}$, $\mathbf{U} \in \mathbb{R}^{d \times K}$ allows a rotation and satisfies $\mathbf{U}^T \mathbf{U} = \mathbf{I}_K$, \mathbf{I}_K is the identity matrix, and $\mathbf{1}_K$ is an all-ones vector.

All vectors in a simplex ETF have an equal ℓ_2 norm and the same pair-wise angle, i.e.,

$$\mathbf{m}_i^T \mathbf{m}_j = \frac{K}{K-1} \delta_{i,j} - \frac{1}{K-1}, \forall i, j \in [1, K], \quad (2)$$

where $\delta_{i,j}$ equals to 1 when $i = j$ and 0 otherwise. The pair-wise angle $-\frac{1}{K-1}$ is the maximal equiangular separation of K vectors in \mathbb{R}^d [4].

Then the neural collapse can be formally described as:

(NC1) Within-class variability of the last-layer features collapse: $\Sigma_W \rightarrow \mathbf{0}$, where $\Sigma_W := \text{Avg}_{i,k} \{(\mathbf{h}_{k,i} - \mathbf{h}_k)(\mathbf{h}_{k,i} - \mathbf{h}_k)^T\}$, where $\mathbf{h}_{k,i}$ is the last-layer feature of the i -th sample in the k -th class, and \mathbf{h}_k is the within-class mean of the last-layer features in the k -th class;

(NC2) Convergence to a simplex ETF: $\tilde{\mathbf{h}}_k = (\mathbf{h}_k - \mathbf{h}_G)/\|\mathbf{h}_k - \mathbf{h}_G\|$, $k \in [1, K]$, satisfies Eq. (2), where \mathbf{h}_G is the global mean of the last-layer features;

(NC3) Self duality: $\tilde{\mathbf{h}}_k = \mathbf{w}_k/\|\mathbf{w}_k\|$, where \mathbf{w}_k is the classifier vector of the k -th class;

(NC4) Simplification to the nearest class center prediction: $\arg\min_k \langle \mathbf{h}, \mathbf{w}_k \rangle = \arg\min_k \|\mathbf{h} - \mathbf{h}_k\|$, where \mathbf{h} is the last-layer feature of a sample to predict for classification.

3.2 Layer-peeled Model

Neural collapse has attracted a lot of researchers to unveil the physics of such an elegant phenomenon. Currently most studies target the cross entropy loss function that is widely used in deep learning for classification and can be described as:

$$\mathcal{L}_{CE}(\mathbf{h}, \mathbf{W}) = -\log \left(\frac{\exp(\mathbf{h}^T \mathbf{w}_c)}{\sum_{k=1}^K \exp(\mathbf{h}^T \mathbf{w}_k)} \right), \quad (3)$$

where $\mathbf{h} \in \mathbb{R}^d$ is the feature output by a backbone network with input \mathbf{x} , $\mathbf{W} = [\mathbf{w}_1, \dots, \mathbf{w}_K] \in \mathbb{R}^{d \times K}$ is a learnable classifier, and c is the class label of \mathbf{x} .

However, deep neural network as a highly interacted function is difficult to analyze due to its non-convexity. A simplification is always necessary to make tractable analysis. For neural collapse, current studies often consider the case that only the last-layer features and classifier are learnable without considering the layers in the backbone network, termed as the layer-peeled model (LPM) [5]. It can be defined as ¹:

$$\begin{aligned} \min_{\mathbf{W}, \mathbf{H}} \quad & \frac{1}{N} \sum_{k=1}^K \sum_{i=1}^{n_k} \mathcal{L}_{CE}(\mathbf{h}_{k,i}, \mathbf{W}), \\ \text{s.t.} \quad & \|\mathbf{w}_k\|^2 \leq E_W, \quad \forall 1 \leq k \leq K, \\ & \|\mathbf{h}_{k,i}\|^2 \leq E_H, \quad \forall 1 \leq k \leq K, 1 \leq i \leq n_k, \end{aligned} \quad (4)$$

where $\mathbf{h}_{k,i}$ is the feature of the i -th sample in the k -th class, \mathbf{W} is a learnable classifier, \mathcal{L}_{CE} is the cross entropy loss function defined in Eq. (3), N is the number of samples, and E_W and E_H are the ℓ_2 norm constraints for feature \mathbf{h} and classifier vector \mathbf{w} , respectively.

Albeit the LPM cannot be applied to real application problems, it serves as an analytical tool and inherits the learning behaviors of the last-layer features and classifier in deep neural network. Actually, the learning of a backbone network is through the multiplication between the Jacobian and the gradient with respect to the last-layer features, *i.e.*, $\frac{\partial \mathbf{H}}{\partial \mathbf{W}_{1:L-1}} \frac{\partial \mathcal{L}}{\partial \mathbf{H}}$, where $\mathbf{W}_{1:L-1}$ denotes the parameters in the backbone network, and \mathbf{H} is the collection of the last-layer features.

It has been shown that the LPM in Eq. (4) has the neural collapse solution as its global optimality in the balanced case. We quote this result as follow:

Theorem 1 (Layer-peeled model in the balanced case [5, 9]) *In the balanced case, *i.e.*, $n_k = n, \forall 1 \leq k \leq K$, any global minimizer $\mathbf{W}^* = [\mathbf{w}_1^*, \dots, \mathbf{w}_K^*]$ and $\mathbf{H}^* = [\mathbf{h}_{k,i}^* : 1 \leq k \leq K, 1 \leq i \leq n]$ of Eq. (4) obeys to neural collapse, *i.e.*,*

$$\frac{\mathbf{h}_{k,i}^*}{\sqrt{E_H}} = \frac{\mathbf{w}_k^*}{\sqrt{E_W}} = \mathbf{m}_k^*, \quad \forall 1 \leq k \leq K, 1 \leq i \leq n, \quad (5)$$

where $\mathbf{M}^* = [\mathbf{m}_1^*, \dots, \mathbf{m}_K^*]$ forms a simplex equiangular tight frame as defined in Eq. (1).

Proof 1 Please refer to [5, 9] for the proof. □

4 Main Results

4.1 ETF Classifier

It has been shown that the neural collapse solution (NC1) minimizes the within-class covariance Σ_W , and (NC2) maximizes the between-class covariance Σ_B by the ETF structure. So the Fisher discriminant ratio, defined as $\Sigma_W^{-1} \Sigma_B$, is maximized, which can measure the linear separability and has been used to extract features to replace the CE loss [32]. So we deem an ETF as the optimal geometric structure for the linear classifier. Considering that a backbone network is usually over-parameterized and can produce features align with any direction, in this paper, we study the potential of learning a network with the linear classifier fixed as an ETF, named ETF classifier.

¹Note that the sample-wise constraint of \mathbf{H} and the class-wise constraint of \mathbf{W} in Eq. (4) are more strict than the overall constraints in [5], but are still active with the same global optimality. The model is also known as unconstrained feature model [6, 10] when the norm constraints are omitted or replaced by regularizations.

Concretely, we initialize the linear classifier \mathbf{W} as a random simplex ETF by Eq. (1) with a scaling of $\sqrt{E_W}$ as the fixed length for each classifier vector, and only optimize the features \mathbf{H} . In this case, the layer-peeled model (LPM) of Eq. (4) reduces to the following problem:

$$\begin{aligned} \min_{\mathbf{H}} \quad & \frac{1}{N} \sum_{k=1}^K \sum_{i=1}^{n_k} \mathcal{L}_{CE}(\mathbf{h}_{k,i}, \mathbf{W}^*), \\ \text{s.t.} \quad & \|\mathbf{h}_{k,i}\|^2 \leq E_H, \quad \forall 1 \leq k \leq K, 1 \leq i \leq n_k, \end{aligned} \quad (6)$$

where \mathbf{W}^* is the fixed classifier as a simplex ETF and satisfies:

$$\mathbf{w}_k^{*T} \mathbf{w}_{k'}^* = E_W \left(\frac{K}{K-1} \delta_{k,k'} - \frac{1}{K-1} \right), \quad \forall k, k' \in [1, K], \quad (7)$$

where $\delta_{k,k'}$ equals to 1 when $k = k'$ and 0 otherwise.

It is observed that this implementation decouples the multiplied learnable variables $\mathbf{h}_{k,i}$ and \mathbf{w}_k of LPM in Eq. (4), and makes the model in Eq. (6) a convex problem that is more tractable. We term the decoupled LPM in Eq. (6) as **DLPM** for short. We have the global optimality of DLPM in the imbalanced case with the ETF classifier in the following theorem.

Theorem 2 *No matter the data distribution is balanced or not among classes (it is allowed that $\exists k, k' \in [1, K], k \neq k'$, such that $n_k \neq n_{k'}$), any global minimizer $\mathbf{H}^* = [\mathbf{h}_{k,i}^* : 1 \leq k \leq K, 1 \leq i \leq n_k]$ of Eq. (6) converges to a simplex ETF with the same direction as \mathbf{W}^* and a length of $\sqrt{E_H}$, i.e.,*

$$\mathbf{h}_{k,i}^{*T} \mathbf{w}_{k'}^* = \sqrt{E_H E_W} \left(\frac{K}{K-1} \delta_{k,k'} - \frac{1}{K-1} \right), \quad (8)$$

for all $1 \leq k, k' \leq K, 1 \leq i \leq n_k$, which means the neural collapse phenomenon emerges.

Proof 2 Please refer to Appendix A for our proof. \square

Remark 1 As observed in [5], LPM in the extreme imbalance case would suffer from “minority collapse”, where the classifier vectors of minor classes are close or even merged into the same vector, which explains the deteriorated classification performance with imbalanced training data. As a comparison, Theorem 2 shows that DLPM with our ETF classifier can inherently produce the neural collapse solution even in the training on imbalanced data.

Although our practice of using a fixed ETF classifier simplifies the problem, it actually brings theoretical merits that also get validated in our long-tailed classification experiments.

4.2 Rethinking the Cross Entropy Loss

In this subsection, we rethink the CE loss from the perspective of gradients with respect to feature and classifier to analyze its learning behaviors.

4.2.1 Gradient *w.r.t* Classifier

We first analyze the gradient of CE loss \mathcal{L}_{CE} *w.r.t* a learnable classifier $\mathbf{W} = [\mathbf{w}_1, \dots, \mathbf{w}_K] \in \mathbb{R}^{d \times K}$:

$$\frac{\partial \mathcal{L}_{CE}}{\partial \mathbf{w}_k} = \sum_{i=1}^{n_k} -(1 - p_k(\mathbf{h}_{k,i})) \cdot \mathbf{h}_{k,i} + \sum_{k' \neq k} \sum_{j=1}^{n_{k'}} p_k(\mathbf{h}_{k',j}) \cdot \mathbf{h}_{k',j}, \quad (9)$$

where $p_k(\mathbf{h})$ is the predicted probability that \mathbf{h} belongs to the k -th class and takes the following form in the CE loss:

$$p_k(\mathbf{h}) = \frac{\exp(\mathbf{h}^T \mathbf{w}_k)}{\sum_{k'=1}^K \exp(\mathbf{h}^T \mathbf{w}_{k'})}, \quad 1 \leq k \leq K. \quad (10)$$

We make the following definitions:

$$-\frac{\partial \mathcal{L}_{CE}}{\partial \mathbf{w}_k} = \mathbf{F}_{\text{pull}}^{(\mathbf{w})} + \mathbf{F}_{\text{push}}^{(\mathbf{w})}, \quad (11)$$

where

$$\begin{aligned} \mathbf{F}_{\text{pull}}^{(\mathbf{w})} &= \sum_{i=1}^{n_k} (1 - p_k(\mathbf{h}_{k,i})) \cdot \mathbf{h}_{k,i}, \\ \mathbf{F}_{\text{push}}^{(\mathbf{w})} &= - \sum_{k' \neq k}^K \sum_{j=1}^{n_{k'}} p_k(\mathbf{h}_{k',j}) \cdot \mathbf{h}_{k',j}. \end{aligned} \quad (12)$$

It reveals that the negative gradient *w.r.t* \mathbf{w}_k is decomposed into two terms. The “pull” term $\mathbf{F}_{\text{pull}}^{(\mathbf{w})}$ pulls \mathbf{w}_k towards the direction of features of the same class, *i.e.*, $\mathbf{h}_{k,i}$, while the “push” term $\mathbf{F}_{\text{push}}^{(\mathbf{w})}$ pushes \mathbf{w}_k away from the direction of features of the other classes *i.e.*, $\mathbf{h}_{k',i}$, $\forall k' \neq k$.

However, note that $\mathbf{F}_{\text{pull}}^{(\mathbf{w})}$ and $\mathbf{F}_{\text{push}}^{(\mathbf{w})}$ have different magnitudes. When the dataset is in extreme imbalance, the direction of $-\frac{\partial \mathcal{L}_{CE}}{\partial \mathbf{w}_k}$ for minor classes is dominated by the push term $\mathbf{F}_{\text{push}}^{(\mathbf{w})}$ because n_k is small, while $N - n_k$ is large. In this case, the classifier vectors of two minor classes are optimized towards nearly the same direction and would be close or merged after training. **So minority collapse results from the imbalanced gradient *w.r.t* classifier in the CE loss. As a comparison, our proposed practice of fixing the classifier as an ETF does not suffer from this dilemma.**

4.2.2 Gradient *w.r.t* Feature

The gradient of CE loss in Eq. (3) with respect to \mathbf{h} is:

$$\frac{\partial \mathcal{L}_{CE}}{\partial \mathbf{h}} = -(1 - p_c(\mathbf{h})) \mathbf{w}_c + \sum_{k \neq c}^K p_k(\mathbf{h}) \mathbf{w}_k, \quad (13)$$

where c is the class label of \mathbf{h} , and $p_k(\mathbf{h})$ is the probability that \mathbf{h} belongs to the k -th class as defined in Eq. (10).

It is shown that Eq. (13) has a similar form to that of Eq. (9). The negative gradient $-\frac{\partial \mathcal{L}_{CE}}{\partial \mathbf{h}}$ can also be decomposed as the addition of $\mathbf{F}_{\text{pull}}^{(\mathbf{h})}$ and $\mathbf{F}_{\text{push}}^{(\mathbf{h})}$ defined as:

$$\begin{aligned} \mathbf{F}_{\text{pull}}^{(\mathbf{h})} &= (1 - p_c(\mathbf{h})) \mathbf{w}_c, \\ \mathbf{F}_{\text{push}}^{(\mathbf{h})} &= - \sum_{k \neq c}^K p_k(\mathbf{h}) \mathbf{w}_k. \end{aligned} \quad (14)$$

The “pull” term $\mathbf{F}_{\text{pull}}^{(\mathbf{h})}$ pulls \mathbf{h} towards the classifier vector of the same class, *i.e.*, \mathbf{w}_c , while the “push” term $\mathbf{F}_{\text{push}}^{(\mathbf{h})}$ pushes \mathbf{h} away from the other classifier vectors, *i.e.*, \mathbf{w}_k , $\forall k \neq c$.

We note that Eq. (12) and Eq. (14) have very symmetric forms. The “pull” terms $\mathbf{F}_{\text{pull}}^{(\mathbf{w})}$ and $\mathbf{F}_{\text{pull}}^{(\mathbf{h})}$ force \mathbf{w} and \mathbf{h} of the same classes to converge to the same direction, which is in line with (NC1) and (NC3). The “push” terms $\mathbf{F}_{\text{push}}^{(\mathbf{w})}$ and $\mathbf{F}_{\text{push}}^{(\mathbf{h})}$ make them of different classes separated, which is in line with (NC2). Generally, (NC1)-(NC3) can lead to (NC4). **We remark that it is the “pull-push” mechanism in the CE loss that produces the neural collapse solution in the case of training on balanced data.**

However, although the “push” term $\mathbf{F}_{\text{push}}^{(\mathbf{h})}$ in Eq. (14) does not cause the imbalance like what $\mathbf{F}_{\text{push}}^{(\mathbf{w})}$ does in Eq. (12), as shown Figure 2, we point out that the direction of $\mathbf{F}_{\text{push}}^{(\mathbf{h})}$ may be inaccurate

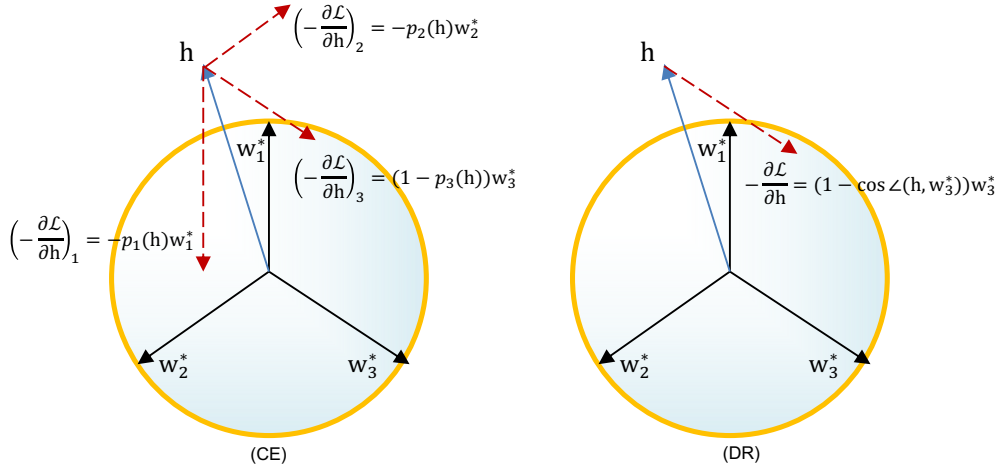


Figure 2: An empirical comparison of gradient directions *w.r.t* an \mathbf{h} (belongs to the 3-rd class) of the CE loss (left) and our proposed DR loss (right). Because \mathbf{h} is close to \mathbf{w}_1^* , the gradient of the CE loss is dominated by $(-\frac{\partial \mathcal{L}_{CE}}{\partial \mathbf{h}})_1$ whose direction deviates from the optimality \mathbf{w}_3^* , while the gradient of DR always directs to \mathbf{w}_3^* .

in our case where the classifier has been fixed as the ETF optimality. Since $\mathbf{F}_{\text{pull}}^{(\mathbf{h})}$ in our case is always accurate towards the optimality \mathbf{w}_c^* , we no longer need the “push” term $\mathbf{F}_{\text{push}}^{(\mathbf{h})}$, which inspires us to develop a new loss function specified for our ETF classifier.

4.3 Dot-Regression Loss

We consider the following squared loss function:

$$\mathcal{L}_{DR}(\mathbf{h}, \mathbf{W}^*) = \frac{1}{2\sqrt{E_W E_H}} \left(\mathbf{w}_c^{*T} \mathbf{h} - \sqrt{E_W E_H} \right)^2, \quad (15)$$

where c is the class label of \mathbf{h} , \mathbf{W}^* is a fixed ETF classifier, and E_W and E_H are the ℓ_2 -norm constraints (predefined and not learnable) given in Eq. (6). It performs regression between the dot product of \mathbf{h} and \mathbf{w}_c^* and the multiplication of their lengths. We term this simple loss function as dot-regression (DR) loss. Its gradient with respect to \mathbf{h} takes the form:

$$\frac{\partial \mathcal{L}_{DR}}{\partial \mathbf{h}} = -(1 - \cos \angle(\mathbf{h}, \mathbf{w}_c^*)) \mathbf{w}_c^*, \quad (16)$$

where $\cos \angle(\mathbf{h}, \mathbf{w}_c^*)$ denotes the cosine distance between \mathbf{h} and \mathbf{w}_c^* .

We see that the gradient has a similar form to the first term in Eq. (13), which plays the role of “pull”, but has no “push” term. It is easy to identify that if we replace the CE loss in the decoupled layer-peeled model (DLPM) defined in Eq. (6) with the DR loss defined in Eq. (15), the same global minimizer Eq. (8) still holds. The global optimality happens when $\mathcal{L}_{DR}(\mathbf{h}^*, \mathbf{W}^*) = 0$ and $\cos \angle(\mathbf{h}^*, \mathbf{w}_c^*) = 1$ accordingly. Then we give a formal analysis of the convergence properties of both CE and DR loss functions in the DLPM.

Definition 2 Given $\delta > 0$, for any \mathbf{h} satisfying $\|\mathbf{h} - \mathbf{h}^*\| \leq \delta$ and $\|\mathbf{h}\|^2 = E_H$, the η -regularity number of function $\mathcal{L}(\mathbf{h})$ is defined by the convergence rate of the projected gradient method. That is, there exists $\eta_{\mathbf{h}} \in [0, 1]$ such that:

$$\|\text{Proj}_{E_H}(\mathbf{h} - \gamma \frac{\partial \mathcal{L}}{\partial \mathbf{h}}) - \mathbf{h}^*\|^2 \leq \eta_{\mathbf{h}} \|\mathbf{h} - \mathbf{h}^*\|^2,$$

where γ is the learning rate such that $\eta_{\mathbf{h}}$ is as small as possible.

Note that $\eta_{\mathbf{h}}$ is decided by \mathbf{h} . For many problems, we cannot find its uniform upper bound $\eta_{\mathbf{h}} \leq \bar{\eta} < 1$. The smaller $\eta_{\mathbf{h}}$ is, the better property the loss function has.

Theorem 3 Assume that given a small $\delta > 0$, when $\|\mathbf{h} - \mathbf{h}^*\| \leq \delta$, $p(\mathbf{h})$ defined in Eq. (10) satisfies that² $p_k(\mathbf{h}) = (1 - p_c(\mathbf{h})) / (K - 1)$, $\forall k \neq c$, where c is the label of \mathbf{h} . When optimizing the DLPM defined in Eq. (6) with the CE and DR loss functions, for any fixed learning rate γ , we have:

$$\eta_{\mathbf{h}}^{(CE)} \geq \frac{1 + \cos \angle(\mathbf{h}, \mathbf{w}_c^*)}{2} = \eta_{\mathbf{h}}^{(DR)}, \quad (17)$$

where $\eta_{\mathbf{h}}^{(CE)}$ and $\eta_{\mathbf{h}}^{(DR)}$ are the η -regularity numbers of the CE and DR loss functions, respectively.

Proof 3 Please refer to Appendix B for our proof. \square

4.4 Implementation

In implementations, we train a backbone network with our proposed ETF classifier and DR loss. We simply perform an ℓ_2 normalization for the features output from the backbone network, which means $\sqrt{E_H} = 1$. Our analytical work has shown that using a fixed ETF classifier does not suffer from the imbalanced gradient *w.r.t* classifier. In implementations, we still need to consider the gradient *w.r.t* the backbone network parameters $\mathbf{W}_{1:L-1}$:

$$\begin{aligned} \frac{1}{N} \frac{\partial \mathcal{L}_{DR}}{\partial \mathbf{W}_{1:L-1}} &= \frac{1}{N} \frac{\partial \mathbf{H}}{\partial \mathbf{W}_{1:L-1}} \frac{\partial \mathcal{L}_{DR}}{\partial \mathbf{H}} \\ &= \frac{1}{N} \sum_{k=1}^K \sum_{i=1}^{n_k} \frac{\partial \mathbf{h}_{k,i}}{\partial \mathbf{W}_{1:L-1}} \frac{\partial \mathcal{L}_{DR}}{\partial \mathbf{h}_{k,i}}. \end{aligned}$$

Then we have:

$$\begin{aligned} \frac{1}{N} \left\| \frac{\partial \mathcal{L}_{DR}}{\partial \mathbf{W}_{1:L-1}} \right\|_2 &\leq \frac{1}{N} \sum_{k=1}^K \sum_{i=1}^{n_k} \left\| \frac{\partial \mathbf{h}_{k,i}}{\partial \mathbf{W}_{1:L-1}} \frac{\partial \mathcal{L}_{DR}}{\partial \mathbf{h}_{k,i}} \right\|_2 \\ &\leq \frac{1}{N} \sum_{k=1}^K \sum_{i=1}^{n_k} \left\| \frac{\partial \mathbf{h}_{k,i}}{\partial \mathbf{W}_{1:L-1}} \right\|_2 \cdot \left\| \frac{\partial \mathcal{L}_{DR}}{\partial \mathbf{h}_{k,i}} \right\|_2 \\ &\leq \frac{2}{N} \sum_{k=1}^K \sum_{i=1}^{n_k} \sigma_{\max} \sqrt{E_{\mathbf{w}_k}}, \end{aligned}$$

where σ_{\max} denotes the largest singular value of the Jacobian $\frac{\partial \mathbf{h}_{k,i}}{\partial \mathbf{W}_{1:L-1}}$, $\forall 1 \leq k \leq K, 1 \leq i \leq n_k$, $\sqrt{E_{\mathbf{w}_k}}$ is the length of the k -th classifier vector, and $\left\| \frac{\partial \mathcal{L}_{DR}}{\partial \mathbf{h}_{k,i}} \right\|_2 \leq 2\sqrt{E_{\mathbf{w}_k}}$ by Eq. (16). Although we cannot realize a balanced gradient *w.r.t* $\mathbf{W}_{1:L-1}$ among classes, we can balance the upper bound of its gradient norm of each class by controlling $\sqrt{E_{\mathbf{w}_k}}$. In implementations, we set $\sqrt{E_{\mathbf{w}_k}} = \frac{N}{Kn_k}$, which is equivalent to performing a weighted loss function on different classes. In experiments, we also compare our method with the weighted CE loss for fair comparison.

5 Experiments

In experiments, we first make empirical observations of neural collapse convergence in the imbalanced training with and without our method, and then compare the performances on long-tailed classification. As an extension, we surprisingly find that our method is also able to improve the performance of fine-grained classification, which can be also deemed as an imbalanced problem where a majority of features are close to each other. The datasets and training details are described in Appendix C.

²Its rational lies in that \mathbf{h}^* aligned with \mathbf{w}_c^* has equal dot products with \mathbf{w}_k^* , $\forall k \neq c$, and \mathbf{h} is close to \mathbf{h}^* .

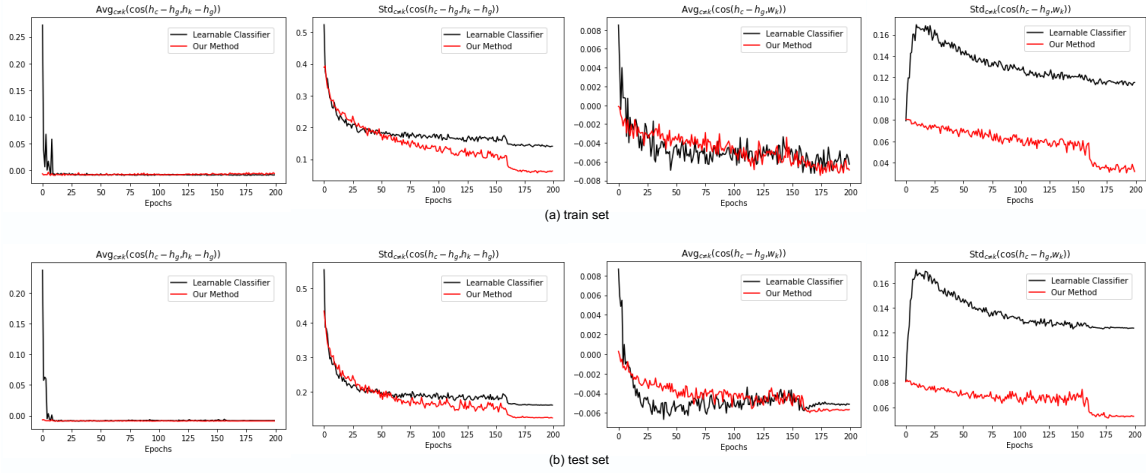


Figure 3: Averages and standard deviations of $\cos \angle(\mathbf{h}_c - \mathbf{h}_g, \mathbf{h}_k - \mathbf{h}_g)$ (two columns on the left), and $\cos \angle(\mathbf{h}_c - \mathbf{h}_g, \mathbf{w}_k)$ (two columns on the right), where \mathbf{h}_g is the global mean, \mathbf{h}_c is the within-class mean, c and k are all pairs of **different** classes, with (red) and without (black) our method on train set (a) and test set (b). The models are trained on CIFAR-100 with an imbalance ratio of 0.02, which is defined as $\frac{n_{\min}}{n_{\max}}$, where n_{\min} and n_{\max} are the minimal and maximal numbers of training samples in all classes.

5.1 Empirical Results

Following [4], we calculate statistics during training to show the neural collapse convergence. We first compare the averages and standard deviations of two cosine similarities, $\cos \angle(\mathbf{h}_c - \mathbf{h}_g, \mathbf{h}_k - \mathbf{h}_g)$ and $\cos \angle(\mathbf{h}_c - \mathbf{h}_g, \mathbf{w}_k)$, where \mathbf{h}_g is the global mean, for all pairs of different classes $(c, k), c \neq k$, with and without our method. As shown in Figure 3, the averages of both $\cos \angle(\mathbf{h}_c - \mathbf{h}_g, \mathbf{h}_k - \mathbf{h}_g)$ and $\cos \angle(\mathbf{h}_c - \mathbf{h}_g, \mathbf{w}_k)$ converge to a negative value near zero. It is consistent with neural collapse that the feature means or classifier vectors of different classes should have a cosine distance of $-\frac{1}{K-1}$. However, their standard deviations are much smaller when our method is used. It indicates that the two models are both trained towards the neural collapse state, while the one with our method converges more closely.

We further calculate the averages of $\cos \angle(\mathbf{h}_c - \mathbf{h}_g, \mathbf{w}_c), \forall 1 \leq c \leq K$, and $\|\tilde{\mathbf{W}} - \tilde{\mathbf{H}}\|_F^2$ as shown in Figure 4 and Figure 5. It reveals that the model using our method generally has a higher $\cos \angle(\mathbf{h}_c - \mathbf{h}_g, \mathbf{w}_c)$ and a lower $\|\tilde{\mathbf{W}} - \tilde{\mathbf{H}}\|_F^2$, which indicates that the feature means and classifier vectors of the same class are better aligned. We observe no advantage of ResNet on STL-10 and DenseNet on CIFAR-100 in Figure 4 and 5. In Table 2, we see that the two cases are right the failure cases, which shows consistency between neural collapse convergence and performance.

5.2 Performances on Long-tailed Classification

We conduct an ablation study with ResNet on CIFAR-10. As shown in Table 1, when we replace the learnable classifier with our fixed ETF classifier, the performances get improved for the imbalance ratio τ of 0.01 and 0.02 without Mixup [33]. They also achieve comparable results for $\tau = 0.1$ and the balanced setting ($\tau = 1$). However, only using the ETF classifier does not work for the extreme imbalance case where $\tau = 0.005$. Besides, it is not compatible with Mixup, which is a strong augmentation tool to alleviate the bias brought by adversarial training samples. When the DR

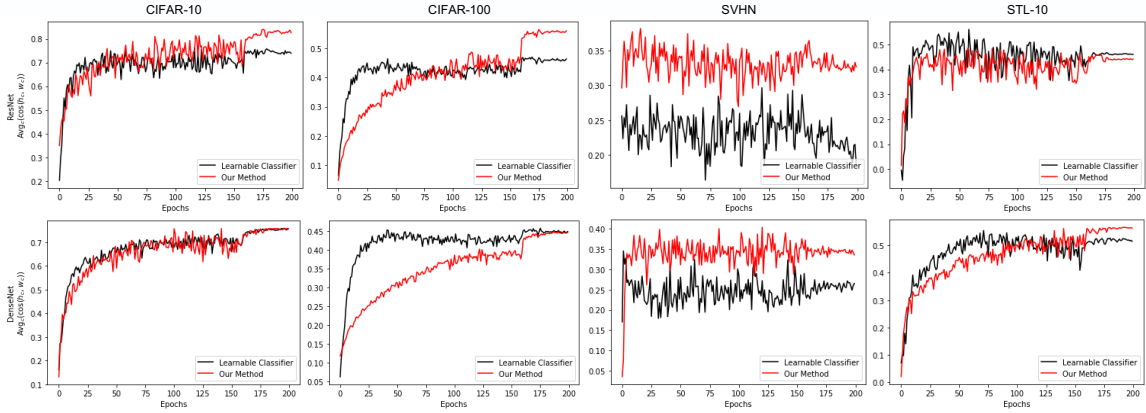


Figure 4: Averages of $\cos \angle(\mathbf{h}_c - \mathbf{h}_g, \mathbf{w}_c)$, $\forall 1 \leq c \leq K$, where \mathbf{h}_g is the global mean, with (red) and without (black) our method, using ResNet (up) and DenseNet (bottom) on four datasets. The models are trained on CIFAR-100 with an imbalance ratio of 0.02.

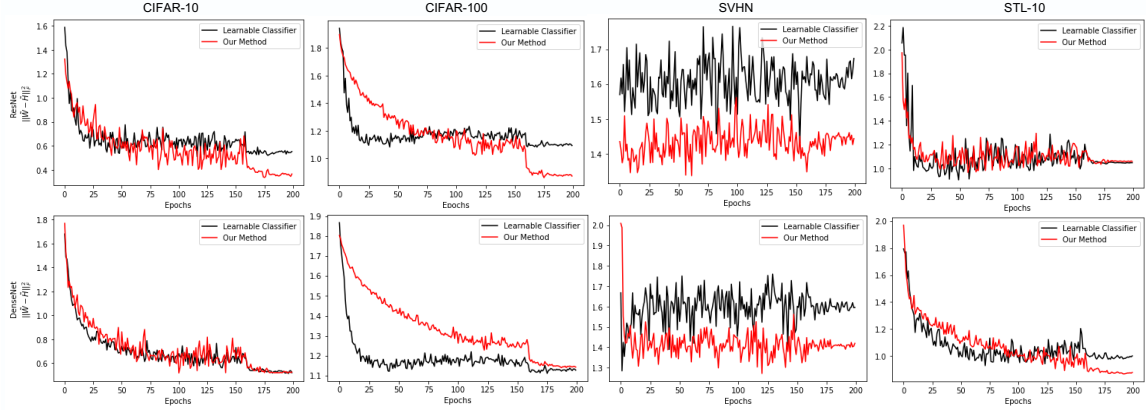


Figure 5: Statistics of $\|\tilde{\mathbf{W}} - \tilde{\mathbf{H}}\|_F^2$ during training, where $\tilde{\mathbf{W}} = \mathbf{W}/\|\mathbf{W}\|_F^2$, $\tilde{\mathbf{H}} = \bar{\mathbf{H}}/\|\bar{\mathbf{H}}\|_F^2$, and $\bar{\mathbf{H}} = [\mathbf{h}_c - \mathbf{h}_g : c = 1, \dots, K]$, using ResNet (up) and DenseNet (bottom) on four datasets. The models are trained on CIFAR-100 with an imbalance ratio of 0.02

loss that is specifically designed for the ETF classifier is used, we achieve significant performance improvements for τ of 0.005, 0.01, and 0.02 with Mixup enabled. It also works for the extreme imbalance case, $\tau = 0.005$, without Mixup. Generally our proposed ETF classifier with the DR loss has better performances on multiple long-tailed cases than the learnable classifier with the original or weighted CE loss. In Table 2, the advantage of our method is further verified on more datasets with both ResNet and DenseNet. Concretely, we achieve an average improvement of 2.0% for ResNet and 1.3% for DenseNet. We find that the failure cases, ResNet on STL-10 and DenseNet on CIFAR-100, correspond to the empirical results shown in Figure 4 and 5.

Table 1: An ablation study with ResNet on CIFAR-10 using different classifiers and loss functions. The numbers in the second row denote the imbalance ratio $\tau = \frac{n_{\min}}{n_{\max}}$, where n_{\min} and n_{\max} are the minimal and maximal numbers of training samples of all classes. Results are the mean of three repeated experiments with different seeds. * indicates that the CE loss is weighted by $\frac{1}{Kn_k}$ to induce class balance, where K is the number of classes and n_k is the number of samples in class k .

Methods	without Mixup					with Mixup				
	0.005	0.01	0.02	0.1	balanced	0.005	0.01	0.02	0.1	balanced
Learnable Classifier + CE	66.1	71.0	77.1	87.4	93.4	67.3	72.8	78.6	87.7	93.6
Learnable Classifier + CE*	66.8	72.1	77.6	87.4	93.1	68.5	73.9	79.3	87.8	93.2
ETF Classifier + CE	60.4	72.9	79.5	87.2	92.6	60.6	67.0	77.2	87.0	93.3
ETF Classifier + DR	68.4	73.0	78.4	86.9	92.9	71.9	76.5	81.0	87.7	92.0

Table 2: Long-tailed classification accuracies (%) with ResNet and DenseNet on four datasets. Mixup is used as default. Results are the mean of three repeated experiments with different seeds.

Methods	CIFAR-10			CIFAR-100			SVHN			STL-10		
	0.005	0.01	0.02	0.005	0.01	0.02	0.005	0.01	0.02	0.005	0.01	0.02
<i>ResNet</i>												
Learnable Classifier + CE	67.3	72.8	78.6	38.7	43.0	48.1	40.5	40.9	49.3	33.1	37.9	38.8
ETF Classifier + DR	71.9	76.5	81.0	40.9	45.3	50.4	42.8	45.7	49.8	33.5	37.2	37.9
Improvements	+4.6	+3.7	+2.4	+2.2	+2.3	+2.3	+2.3	+4.8	+0.5	+0.4	-0.7	-0.9
<i>DenseNet</i>												
Learnable Classifier + CE	63.0	69.7	76.1	40.3	43.8	49.8	39.7	40.5	46.4	38.5	41.2	44.9
ETF Classifier + DR	65.7	71.6	75.8	40.1	44.0	49.7	40.5	44.8	48.4	39.5	42.9	46.3
Improvements	+2.7	+1.9	-0.3	-0.2	+0.2	-0.1	+0.8	+4.3	+2.0	+1.0	+1.7	+1.4

Table 3: Fine-grained classification accuracies (%) on CUB-200-2011 with ResNet backbone networks pre-trained on ImageNet.

Methods	Accuracy (%)
<i>ResNet-34</i>	
Learnable Classifier + CE loss	82.2
ETF Classifier + DR loss	83.0
Improvements	+0.8
<i>ResNet-50</i>	
Learnable Classifier + CE loss	85.5
ETF Classifier + DR loss	86.1
Improvements	+0.6
<i>ResNet-101</i>	
Learnable Classifier + CE loss	86.2
ETF Classifier + DR loss	87.0
Improvements	+0.8

5.3 Performances on Fine-grained Classification

Fine-grained classification can also be deemed as an imbalanced problem as the features of multiple classes are close to each other. We surprisingly find that our method is also helpful for fine-grained classification even though most of the analytical work is conducted under the case of class imbalance. As shown in Table 3, our method achieves 0.7%-0.8% accuracy improvements on CUB-200-2011.

6 Conclusion

In this paper, we study the potential of training a network with the last-layer linear classifier randomly initialized as a simplex ETF and fixed during training. This practice enjoys theoretical merits under the layer-peeled analytical framework. We further develop a simple loss function specifically for the ETF classifier. Its advantage gets verified by both theoretical and experimental results. We conclude that it is not necessary to learn a linear classifier for classification networks, and our simplified practice even helps to improve the long-tailed and fine-grained classification problems. Our work may help to further understand neural collapse and deep neural network for classification, and inspire future studies on the design or search of neural architectures.

References

- [1] Yann LeCun, Yoshua Bengio, and Geoffrey Hinton. Deep learning. *Nature*, 521(7553):436–444, 2015.
- [2] Kaiming He, Xiangyu Zhang, Shaoqing Ren, and Jian Sun. Deep residual learning for image recognition. In *CVPR*, pages 770–778, 2016.
- [3] Gao Huang, Zhuang Liu, Laurens Van Der Maaten, and Kilian Q Weinberger. Densely connected convolutional networks. In *CVPR*, pages 4700–4708, 2017.
- [4] Vardan Papyan, XY Han, and David L Donoho. Prevalence of neural collapse during the terminal phase of deep learning training. *Proceedings of the National Academy of Sciences*, 117(40):24652–24663, 2020.
- [5] Cong Fang, Hangfeng He, Qi Long, and Weijie J Su. Exploring deep neural networks via layer-peeled model: Minority collapse in imbalanced training. *Proceedings of the National Academy of Sciences*, 118(43), 2021.
- [6] Dustin G Mixon, Hans Parshall, and Jianzong Pi. Neural collapse with unconstrained features. *arXiv preprint arXiv:2011.11619*, 2020.
- [7] E Weinan and Stephan Wojtowytsch. On the emergence of tetrahedral symmetry in the final and penultimate layers of neural network classifiers. *arXiv preprint arXiv:2012.05420*, 2020.
- [8] Jianfeng Lu and Stefan Steinerberger. Neural collapse with cross-entropy loss. *arXiv preprint arXiv:2012.08465*, 2020.
- [9] Florian Graf, Christoph Hofer, Marc Niethammer, and Roland Kwitt. Dissecting supervised contrastive learning. In *ICML*, pages 3821–3830. PMLR, 2021.
- [10] Zhihui Zhu, Tianyu DING, Jinxin Zhou, Xiao Li, Chong You, Jeremias Sulam, and Qing Qu. A geometric analysis of neural collapse with unconstrained features. In *NeurIPS*, 2021.
- [11] Wenlong Ji, Yiping Lu, Yiliang Zhang, Zhun Deng, and Weijie J Su. An unconstrained layer-peeled perspective on neural collapse. In *ICLR*, 2022.
- [12] XY Han, Vardan Papyan, and David L Donoho. Neural collapse under mse loss: Proximity to and dynamics on the central path. In *ICLR*, 2022.
- [13] Tomaso Poggio and Qianli Liao. Explicit regularization and implicit bias in deep network classifiers trained with the square loss. *arXiv preprint arXiv:2101.00072*, 2020.
- [14] Tom Tirer and Joan Bruna. Extended unconstrained features model for exploring deep neural collapse. *arXiv preprint arXiv:2202.08087*, 2022.
- [15] Ronald A Fisher. The use of multiple measurements in taxonomic problems. *Annals of eugenics*, 7(2):179–188, 1936.
- [16] C Radhakrishna Rao. The utilization of multiple measurements in problems of biological classification. *Journal of the Royal Statistical Society. Series B (Methodological)*, 10(2):159–203, 1948.
- [17] Edouard Oyallon. Building a regular decision boundary with deep networks. In *CVPR*, pages 5106–5114, 2017.
- [18] Vardan Papyan. Traces of class/cross-class structure pervade deep learning spectra. *Journal of Machine Learning Research*, 21(252):1–64, 2020.

- [19] John Zarka, Florentin Guth, and Stéphane Mallat. Separation and concentration in deep networks. In *ICLR*, 2020.
- [20] Adrian FM Smith and David J Spiegelhalter. Bayes factors and choice criteria for linear models. *Journal of the Royal Statistical Society: Series B (Methodological)*, 42(2):213–220, 1980.
- [21] K. Simonyan and A. Zisserman. Very deep convolutional networks for large-scale image recognition. In *ICLR*, 2015.
- [22] Yibo Yang, Zhisheng Zhong, Tiancheng Shen, and Zhouchen Lin. Convolutional neural networks with alternately updated clique. In *CVPR*, pages 2413–2422, 2018.
- [23] Huan Li, Yibo Yang, Dongmin Chen, and Zhouchen Lin. Optimization algorithm inspired deep neural network structure design. *arXiv preprint arXiv:1810.01638*, 2018.
- [24] Sanjeev Arora, Simon Du, Wei Hu, Zhiyuan Li, and Ruosong Wang. Fine-grained analysis of optimization and generalization for overparameterized two-layer neural networks. In *ICML*, pages 322–332. PMLR, 2019.
- [25] Arthur Jacot, Clément Hongler, and Franck Gabriel. Neural tangent kernel: Convergence and generalization in neural networks. In *NeurIPS*, pages 8580–8589, 2018.
- [26] Song Mei, Andrea Montanari, and Phan-Minh Nguyen. A mean field view of the landscape of two-layer neural networks. *Proceedings of the National Academy of Sciences*, 115(33):E7665–E7671, 2018.
- [27] Kaidi Cao, Colin Wei, Adrien Gaidon, Nikos Arechiga, and Tengyu Ma. Learning imbalanced datasets with label-distribution-aware margin loss. In *NeurIPS*, volume 32, 2019.
- [28] Bingyi Kang, Saining Xie, Marcus Rohrbach, Zhicheng Yan, Albert Gordo, Jiashi Feng, and Yannis Kalantidis. Decoupling representation and classifier for long-tailed recognition. In *ICLR*, 2020.
- [29] Zhisheng Zhong, Jiequan Cui, Shu Liu, and Jiaya Jia. Improving calibration for long-tailed recognition. In *CVPR*, pages 16489–16498, 2021.
- [30] Andrew R Webb and David Lowe. The optimised internal representation of multilayer classifier networks performs nonlinear discriminant analysis. *Neural Networks*, 3(4):367–375, 1990.
- [31] Tolga Ergen and Mert Pilanci. Revealing the structure of deep neural networks via convex duality. In *ICML*, pages 3004–3014. PMLR, 2021.
- [32] Andre Stuhlsatz, Jens Lippel, and Thomas Zielke. Feature extraction with deep neural networks by a generalized discriminant analysis. *IEEE Transactions on Neural Networks and Learning Systems*, 23(4):596–608, 2012.
- [33] Hongyi Zhang, Moustapha Cisse, Yann N. Dauphin, and David Lopez-Paz. mixup: Beyond empirical risk minimization. In *ICLR*, 2018.

A Proof for Theorem 2

Note that the constrained optimization problem of Eq. (6) in our case is separable. We consider the k -th ($1 \leq k \leq K$ and $K \geq 2$) problem as:

$$\begin{aligned} \min_{\mathbf{H}} \quad & \frac{1}{N} \sum_{i=1}^{n_k} \mathcal{L}_{CE}(\mathbf{h}_{k,i}, \mathbf{W}^*), \\ \text{s.t.} \quad & \|\mathbf{h}_{k,i}\|^2 \leq E_H, \quad 1 \leq i \leq n_k. \end{aligned} \quad (18)$$

where \mathbf{W}^* is the fixed ETF classifier. The problem above is convex as the objective is a sum of affine functions and log-sum-exp functions with convex constraints. We have the Lagrange function as:

$$\tilde{L} = \frac{1}{N} \sum_{i=1}^{n_k} -\log \frac{\exp(\mathbf{h}_{k,i}^T \mathbf{w}_k^*)}{\sum_{j \neq k} \exp(\mathbf{h}_{k,i}^T \mathbf{w}_j^*)} + \sum_{i=1}^{n_k} \mu_i (\|\mathbf{h}_{k,i}\|^2 - E_H), \quad (19)$$

where μ_i is the Lagrange multiplier. We have its gradient with respect to $\mathbf{h}_{k,i}$ as:

$$\frac{\partial \tilde{L}}{\partial \mathbf{h}_{k,i}} = -\frac{(1-p_k) \mathbf{w}_k^*}{N} + \frac{1}{N} \sum_{j \neq k} p_j \mathbf{w}_j^* + 2\mu_i \mathbf{h}_{k,i}, \quad 1 \leq i \leq n_k. \quad (20)$$

First we consider the case when $\mu_i = 0$. $\partial \tilde{L} / \partial \mathbf{h}_{k,i} = 0$ gives the following equation:

$$\sum_{j \neq k} p_j \mathbf{w}_j^* = \sum_{j \neq k} p_j \mathbf{w}_k^*. \quad (21)$$

Multiplying \mathbf{w}_k^* by both sides of the equation, we should have:

$$\frac{K}{K-1} \sum_{j \neq k} p_j = 0, \quad (22)$$

which contradicts with $p_j > 0, \forall 1 \leq j \leq K$ when the ℓ_2 norm of $\mathbf{h}_{k,i}$ is constrained and \mathbf{W}^* has a fixed ℓ_2 norm. So we have $\mu_i > 0$ and according to the KKT condition:

$$\|\mathbf{h}_{k,i}\|^2 = E_H, \quad (23)$$

Then we have the equation:

$$\frac{\partial \tilde{L}}{\partial \mathbf{h}_{k,i}^*} = \frac{1}{N} \sum_{j \neq k} p_j (\mathbf{w}_j^* - \mathbf{w}_k^*) + 2\mu_i \mathbf{h}_{k,i}^* = 0, \quad (24)$$

where $\mathbf{h}_{k,i}^*$ is the optimal solution of $\mathbf{h}_{k,i}$. Multiplying $\mathbf{w}_{j'}^*$ ($j' \neq k$) by both sides of Eq. (24), we get:

$$E_W p_{j'} \left(1 + \frac{1}{K-1} \right) + 2N\mu_i \langle \mathbf{h}_{k,i}^*, \mathbf{w}_{j'}^* \rangle = 0. \quad (25)$$

Since $p_{j'} > 0$ and $K-1 > 0$, we have $\langle \mathbf{h}_{k,i}^*, \mathbf{w}_{j'}^* \rangle < 0$. Then for any pair $j, j' \neq k$, we have:

$$\frac{p_j}{p_{j'}} = \frac{\exp(\langle \mathbf{h}_{k,i}^*, \mathbf{w}_j^* \rangle)}{\exp(\langle \mathbf{h}_{k,i}^*, \mathbf{w}_{j'}^* \rangle)} = \frac{\langle \mathbf{h}_{k,i}^*, \mathbf{w}_j^* \rangle}{\langle \mathbf{h}_{k,i}^*, \mathbf{w}_{j'}^* \rangle}. \quad (26)$$

Considering that the function $f(x) = \exp(x)/x$ is monotonically increasing when $x < 0$, we have :

$$\langle \mathbf{h}_{k,i}^*, \mathbf{w}_j^* \rangle = \langle \mathbf{h}_{k,i}^*, \mathbf{w}_{j'}^* \rangle = C, \quad p_j = p_{j'} = p, \quad \forall j, j' \neq k, \quad (27)$$

where C and p are constants. From Eq. (25), we have:

$$p = \frac{1-K}{K} \cdot \frac{2N\mu_i C}{E_W}, \quad (28)$$

$$1 - p_k = (K - 1)p = \frac{(1 - K)(K - 1)}{K} \cdot \frac{2N\mu_i C}{E_W}, \quad (29)$$

and

$$1 - p_k + p = (1 - K) \cdot \frac{2N\mu_i C}{E_W}. \quad (30)$$

From Eq. (24), we have:

$$\mathbf{h}_{k,i}^* = \frac{1}{2N\mu_i} \left[(1 - p_k) \mathbf{w}_k^* - \sum_{j \neq k} p_j \mathbf{w}_j^* \right]. \quad (31)$$

The ETF classifier defined in Eq. (1) satisfies that $\sum_i^K \mathbf{w}_i^* = 0$. Given that $p_j = p, \forall j \neq k$ and Eq. (30), we have:

$$\begin{aligned} \mathbf{h}_{k,i}^* &= \frac{1}{2N\mu_i} (1 - p_k + p) \mathbf{w}_k^* \\ &= \frac{(1 - K)C}{E_W} \mathbf{w}_k^*, \end{aligned} \quad (32)$$

which indicates that $\mathbf{h}_{k,i}^*$ has the same direction as \mathbf{w}_k^* . Its length has been given in Eq. (23). Then we have:

$$C = \langle \mathbf{h}_{k,i}^*, \mathbf{w}_j^* \rangle = -\frac{\sqrt{E_H E_W}}{K - 1}, \quad \forall j \neq k, \quad (33)$$

and

$$\mathbf{h}_{k,i}^* = \sqrt{\frac{E_H}{E_W}} \mathbf{w}_k^*, \quad (34)$$

which is equivalent to Eq. (8) and concludes the proof. \square

B Proof for Theorem 3

We would like to show that the $\eta_{\mathbf{h}}$ of \mathcal{L}_{DR} is always smaller than that of \mathcal{L}_{CE} given \mathbf{h}^t is close to \mathbf{h}^* .

For the DR loss: We suppose $\|\mathbf{h}_{k,i}^0\|^2 = E_H$ and $\cos \angle(\mathbf{h}_{k,i}^0, \mathbf{w}_k^*) \geq 0$ for any k, i . For the DR loss in (15), the projected SGD takes the following step at time $t + 1$ with the sample i in the class k .

$$\mathbf{h}_{k,i}^{t+1} = \text{Proj}_{\text{EH}}(\mathbf{h}_{k,i}^t - \gamma \frac{\partial \mathcal{L}_{DR}}{\partial \mathbf{h}_{k,i}}) = \text{Proj}_{\text{EH}}(\mathbf{h}_{k,i}^t - \gamma (\cos \angle(\mathbf{h}_{k,i}^t, \mathbf{w}_k^*) - 1) \mathbf{w}_k^*), \quad (35)$$

where Proj_{EH} is the orthogonal projection onto the ball $\{\mathbf{h} : \|\mathbf{h}\|^2 \leq E_H\}$. Note that $\mathbf{h}_{k,j}^{t+1} = \mathbf{h}_{k,j}^t$ for $j \neq i$ and $\mathbf{h}_{c,j}^{t+1} = \mathbf{h}_{c,j}^t$ for $c \neq k$. One has

$$\|\mathbf{h}_{k,i}^t - \gamma \frac{\partial \mathcal{L}_{DR}}{\partial \mathbf{h}_{k,i}}\|^2 = E_H - 2\sqrt{E_H E_W} \gamma (\cos \angle(\mathbf{h}_{k,i}^t, \mathbf{w}_k^*) - 1) \cos \angle(\mathbf{h}_{k,i}^t, \mathbf{w}_k^*) + \gamma^2 E_W (\cos \angle(\mathbf{h}_{k,i}^t, \mathbf{w}_k^*) - 1)^2 \geq E_H.$$

By the non-expansiveness of projection, one has the following convergence

$$\begin{aligned} \|\mathbf{h}_{k,i}^{t+1} - \mathbf{h}_{k,i}^*\|^2 &\leq \|\mathbf{h}_{k,i}^t - \gamma (\cos \angle(\mathbf{h}_{k,i}^t, \mathbf{w}_k^*) - 1) \mathbf{w}_k^* - \mathbf{h}_{k,i}^*\|^2 \\ &= \|\mathbf{h}_{k,i}^t - \mathbf{h}_{k,i}^*\|^2 - 2\gamma (\cos \angle(\mathbf{h}_{k,i}^t, \mathbf{w}_k^*) - 1) \langle \mathbf{h}_{k,i}^t - \mathbf{h}_{k,i}^*, \mathbf{w}_k^* \rangle + \gamma^2 (\cos \angle(\mathbf{h}_{k,i}^t, \mathbf{w}_k^*) - 1)^2 E_W \\ &= 2E_H (1 - \cos \angle(\mathbf{h}_{k,i}^t, \mathbf{w}_k^*)) - 2\gamma \sqrt{E_H E_W} (\cos \angle(\mathbf{h}_{k,i}^t, \mathbf{w}_k^*) - 1)^2 + \gamma^2 E_W (\cos \angle(\mathbf{h}_{k,i}^t, \mathbf{w}_k^*) - 1)^2. \end{aligned} \quad (36)$$

When $\gamma = \frac{\sqrt{E_H}}{\sqrt{E_W}}$, we have

$$\begin{aligned} \|\mathbf{h}_{k,i}^{t+1} - \mathbf{h}_{k,i}^*\|^2 &\leq 2E_H (1 - \cos \angle(\mathbf{h}_{k,i}^t, \mathbf{w}_k^*)) - E_H (1 - \cos \angle(\mathbf{h}_{k,i}^t, \mathbf{w}_k^*))^2 \\ &= \frac{1 + \cos \angle(\mathbf{h}_{k,i}^t, \mathbf{w}_k^*)}{2} \|\mathbf{h}_{k,i}^t - \mathbf{h}_{k,i}^*\|^2. \end{aligned} \quad (37)$$

Note that combining (35) with (36) implies that $\|\mathbf{h}_{k,i}^t\|^2 = E_H$ and $\cos \angle(\mathbf{h}_{k,i}^t, \mathbf{w}_k^*) \geq 0$ for all $t \geq 0$. We get that the $\eta_{\mathbf{h}}$ -regularity number of the DR loss is

$$\eta_{\mathbf{h}}^{(DR)} = \frac{1 + \cos \angle(\mathbf{h}_{k,i}^t, \mathbf{w}_k^*)}{2}.$$

For the CE loss:

On the other hand, for the CE loss in (3), the projected SGD takes the following step at time $t+1$ with the sample i in the class k .

$$\mathbf{h}_{k,i}^{t+1} = \text{Proj}_{E_H}(\mathbf{h}_{k,i}^t - \gamma \frac{\partial \mathcal{L}^{CE}}{\partial \mathbf{h}_{k,i}}) = \text{Proj}_{E_H} \left(\mathbf{h}_{k,i}^t + \gamma(1-p_k) \mathbf{w}_k^* - \gamma \sum_{j \neq k}^K p_j \mathbf{w}_j^* \right).$$

Note that $\mathbf{h}_{k,j}^{t+1} = \mathbf{h}_{k,j}^t$ for $j \neq i$ and $\mathbf{h}_{c,j}^{t+1} = \mathbf{h}_{c,j}^t$ for $c \neq k$.

One has the following convergence

$$\begin{aligned} \|\mathbf{h}_{k,i}^{t+1} - \mathbf{h}_{k,i}^*\|^2 &\leq \|\mathbf{h}_{k,i}^t + \gamma(1-p_k) \mathbf{w}_k^* - \gamma \sum_{j \neq k}^K p_j \mathbf{w}_j^* - \mathbf{h}_{k,i}^*\|^2 \\ &= \|\mathbf{h}_{k,i}^t - \mathbf{h}_{k,i}^*\|^2 - 2\gamma(p_k - 1) \langle \mathbf{h}_{k,i}^t - \mathbf{h}_{k,i}^*, \mathbf{w}_k^* \rangle + \gamma^2(p_k - 1)^2 E_W \\ &\quad + 2\gamma \left\langle \mathbf{h}_{k,i}^* - \mathbf{h}_{k,i}^t, \sum_{j \neq k}^K p_j \mathbf{w}_j^* \right\rangle \\ &\quad - 2\gamma \left\langle (1-p_k) \gamma \mathbf{w}_k^*, \sum_{j \neq k}^K p_j \mathbf{w}_j^* \right\rangle + \|\gamma \sum_{j \neq k}^K p_j \mathbf{w}_j^*\|^2 \\ &= \|\mathbf{h}_{k,i}^t - \mathbf{h}_{k,i}^*\|^2 + \gamma^2(p_k - 1)^2 E_W + \|\gamma \sum_{j \neq k}^K p_j \mathbf{w}_j^*\|^2 + M, \end{aligned} \tag{38}$$

where we have:

$$\begin{aligned} M &= 2\gamma(1-p_k) \langle \mathbf{h}_{k,i}^t - \mathbf{h}_{k,i}^*, \mathbf{w}_k^* \rangle - 2\gamma \left\langle (1-p_k) \gamma \mathbf{w}_k^*, \sum_{j \neq k}^K p_j \mathbf{w}_j^* \right\rangle + 2\gamma \left\langle \mathbf{h}_{k,i}^* - \mathbf{h}_{k,i}^t, \sum_{j \neq k}^K p_j \mathbf{w}_j^* \right\rangle \\ &= 2\gamma(1-p_k) \left(\langle \mathbf{h}_{k,i}^t - \mathbf{h}_{k,i}^*, \mathbf{w}_k^* \rangle + \frac{\gamma E_W}{K-1} \sum_{j \neq k}^K p_j \right) + 2\gamma \left\langle \mathbf{h}_{k,i}^* - \mathbf{h}_{k,i}^t, \sum_{j \neq k}^K p_j \mathbf{w}_j^* \right\rangle \\ &= 2\gamma(1-p_k) \left(\langle \mathbf{h}_{k,i}^t, \mathbf{w}_k^* \rangle - \sqrt{E_H E_W} + \frac{\gamma E_W (1-p_k)}{K-1} \right) - 2\gamma \mathbf{h}_{k,i}^t \sum_{j \neq k}^K p_j \mathbf{w}_j^* - \frac{2\gamma(1-p_k)}{K-1} \sqrt{E_H E_W} \\ &= 2\gamma(1-p_k) \langle \mathbf{h}_{k,i}^t, \mathbf{w}_k^* \rangle - 2\gamma \mathbf{h}_{k,i}^t \sum_{j \neq k}^K p_j \mathbf{w}_j^* - 2\gamma(1-p_k) \frac{K}{K-1} \sqrt{E_H E_W} + \frac{2\gamma^2(1-p_k)^2 E_W}{K-1}. \end{aligned} \tag{39}$$

Since $\sum_i^K \mathbf{w}_i^* = 0$ for an ETF classifier, and we have the assumption that $p_i = p_j = \frac{1-p_k}{K-1}$, $\forall i, j \neq k$, then we

have:

$$\begin{aligned}
& 2\gamma(1-p_k)\langle \mathbf{h}_{k,i}^t, \mathbf{w}_k^* \rangle - 2\gamma \mathbf{h}_{k,i}^t \sum_{j \neq k}^K p_j \mathbf{w}_j^* \\
&= -2\gamma \langle \mathbf{h}_{k,i}^t, (1-p_k) \sum_{j \neq k}^K \mathbf{w}_j^* + \sum_{j \neq k}^K p_j \mathbf{w}_j^* \rangle \\
&\stackrel{a}{=} -2\gamma \langle \mathbf{h}_{k,i}^t, \frac{K(1-p_k)}{K-1} \sum_{j \neq k}^K \mathbf{w}_j^* \rangle \\
&\stackrel{b}{=} -\frac{2K}{K-1} (1-p_k) \gamma \sqrt{E_H E_W} \left(\sum_{j \neq k}^K \cos \angle(\mathbf{h}_{k,i}^t, \mathbf{w}_j^*) \right) \\
&= \frac{2K}{K-1} (1-p_k) \gamma \sqrt{E_H E_W} \cos \angle(\mathbf{h}_{k,i}^t, \mathbf{w}_k^*),
\end{aligned} \tag{40}$$

where $\stackrel{a}{=}$ follows from $p_i = p_j = \frac{1-p_k}{K-1}$, and $\stackrel{b}{=}$ holds because $\langle \mathbf{h}_{k,i}^t, \sum_i^K \mathbf{w}_i^* \rangle = 0$. Then we have :

$$\begin{aligned}
M &= \frac{2K}{K-1} (1-p_k) \gamma \sqrt{E_H E_W} \cos \angle(\mathbf{h}_{k,i}^t, \mathbf{w}_k^*) - 2(1-p_k) \frac{K}{K-1} E_H + \frac{2\gamma^2 (1-p_k)^2 E_W}{K-1} \\
&= -2(1-p_k) \frac{K}{K-1} \gamma \sqrt{E_H E_W} (1 - \cos \angle(\mathbf{h}_{k,i}^t, \mathbf{w}_k^*)) + \frac{2\gamma^2 (1-p_k)^2 E_W}{K-1},
\end{aligned} \tag{41}$$

and

$$\begin{aligned}
\|\mathbf{h}_{k,i}^{t+1} - \mathbf{h}_{k,i}^*\|^2 &\leq \|\mathbf{h}_{k,i}^t - \mathbf{h}_{k,i}^*\|^2 - \frac{2K\sqrt{E_H E_W}}{K-1} \gamma (1-p_k) (1 - \cos \angle(\mathbf{h}_{k,i}^t, \mathbf{w}_k^*)) + \gamma^2 (p_k - 1)^2 E_W + \\
&\quad \|\gamma \sum_{j \neq k}^K p_j \mathbf{w}_j^*\|^2 + \frac{2\gamma^2 (1-p_k)^2 E_W}{K-1} \\
&= 2E_H (1 - \cos \angle(\mathbf{h}_{k,i}^t, \mathbf{w}_k^*)) - E_H (1 - \cos \angle(\mathbf{h}_{k,i}^t, \mathbf{w}_k^*))^2 + \\
&\quad E_H (1 - \cos \angle(\mathbf{h}_{k,i}^t, \mathbf{w}_k^*))^2 + \frac{2K\sqrt{E_H E_W}}{K-1} \gamma (1-p_k) (1 - \cos \angle(\mathbf{h}_{k,i}^t, \mathbf{w}_k^*)) + \gamma^2 (p_k - 1)^2 E_W + \\
&\quad \frac{\gamma^2 (1-p_k)^2 E_W}{(K-1)^2} + \frac{2\gamma^2 (1-p_k)^2 E_W}{K-1}.
\end{aligned} \tag{42}$$

Let $\gamma(1-p_k) \frac{K}{K-1} = s_k$, and we consider the problem:

$$\min_{s_k} E_H (1 - \cos \angle(\mathbf{h}_{k,i}^t, \mathbf{w}_k^*))^2 - 2\sqrt{E_H E_W} (1 - \cos \angle(\mathbf{h}_{k,i}^t, \mathbf{w}_k^*)) s_k + E_W s_k^2.$$

When $s_k = \sqrt{\frac{E_H}{E_W}} (1 - \cos \angle(\mathbf{h}_{k,i}^t, \mathbf{w}_k^*))$, i.e., $\gamma = \frac{K-1}{K} \sqrt{\frac{E_H}{E_W}} \frac{1 - \cos \angle(\mathbf{h}_{k,i}^t, \mathbf{w}_k^*)}{1-p_k}$, we get the optimal bound for CE as:

$$\begin{aligned}
\|\mathbf{h}_{k,i}^{t+1} - \mathbf{h}_{k,i}^*\|^2 &\leq 2E_H (1 - \cos \angle(\mathbf{h}_{k,i}^t, \mathbf{w}_k^*)) - E_H (1 - \cos \angle(\mathbf{h}_{k,i}^t, \mathbf{w}_k^*))^2 \\
&= \frac{1 + \cos \angle(\mathbf{h}_{k,i}^t, \mathbf{w}_k^*)}{2} \|\mathbf{h}_{k,i}^t - \mathbf{h}_{k,i}^*\|^2,
\end{aligned} \tag{43}$$

which is the same as DR. However, in this case γ varies and cannot be a constant as defined in Definition 2. For any fixed learning rate γ , we have the $\eta_{\mathbf{h}}$ -regularity number of the CE loss:

$$\eta_{\mathbf{h}}^{(CE)} \geq \frac{1 + \cos \angle(\mathbf{h}_{k,i}^t, \mathbf{w}_k^*)}{2} = \eta_{\mathbf{h}}^{(DR)}, \tag{44}$$

and conclude the proof. \square

C Datasets and Training Details

We conduct long-tailed classification experiments on the four datasets, CIFAR-10, CIFAR-100, SVHN, and STL-10, with two models, ResNet-32 and DenseNet with a depth of 100 and a growth rate of 12. All models are trained with the same training setting. Concretely, we train for 200 epochs, with an initial learning rate of 0.1, a batchsize of 128, a momentum of 0.9, and a weight decay of $2e - 4$. The learning rate is divided by 10 at epoch 160 and 180. The hyper-parameter in the β distribution used for Mixup is set as 1.0 when Mixup is used. We use the code released by [29] to produce the imbalanced datasets. The numbers of training samples are decayed exponentially among classes. We adopt the standard data normalization and augmentation for the four datasets.

We conduct fine-grained classification experiments on CUB-200-2011, with ResNet-34, ResNet-50, and ResNet-101. The ResNet backbone networks are pre-trained on ImageNet. We train for 300 epochs on CUB-200-2011 with an initial learning rate of 0.04, and drop the learning rate by 0.1 at epoch 90, 180, and 270. The standard data normalization and augmentation are adopted. Other training settings are the same as the long-tailed experiments.